

Microfabricated Millimeter-Wave High-Power Vacuum Electronic Amplifiers

Colin D. Joye^{a*}, Alan M. Cook^a, Jeffrey P. Calame^a, David K. Abe^a, Khanh T. Nguyen^b, Edward L. Wright^b, Dean E. Pershing^b, and Baruch Levush^a

^aNaval Research Laboratory, Code 6850, Washington, DC 20375 USA

^bBeam-Wave Research, Inc., Bethesda MD 20814 USA

*Contact Author Email: colin.joye@nrl.navy.mil

Abstract: Utilizing a novel ultraviolet photolithography microfabrication technique involving embedded polymer monofilaments, the U.S. Naval Research Laboratory is demonstrating and developing millimeter-wave vacuum electronic traveling wave tube amplifiers at W- and G-band in the 10's to 100's of watts power range at several percent instantaneous bandwidth.

Keywords: Traveling wave tube; millimeter wave; vacuum electron device; microfabrication; photolithography.

Introduction

Ultraviolet photolithography techniques along with copper electroforming (collectively, UV-LIGA) show much promise for fabricating millimeter-wave (mmW) and sub-mmW amplifiers [1-2]. Trends toward higher frequencies come at the expense of more difficult microfabrication, since the electron beam must be transported through ever smaller beam tunnels and tighter tolerances. At 95 GHz and above, CNC machining, electrical discharge machining and other methods are simply not able to hold the tolerances needed for these microfabricated parts. With use of UV-transparent, refractive index-matched polymer monofilaments along with SU-8 mold forming, 3D all-copper structures have been demonstrated that allow extremely high aspect ratio beam tunnels to be fabricated along with the all-copper slow-wave amplifier circuits (Patent Applications filed 2012).

In spite of the challenges, high power sources of electromagnetic radiation are needed in the mmW bands for advanced DoD applications such as ultra wideband communications, long-range imaging, and high-resolution, through-cloud radar. Table 1 shows the current efforts at NRL to meet needs at W-band and G-band.

TABLE I: Amplifier Operating Parameters

	220 GHz	233 GHz	95 GHz
Beam voltage	11.7 kV	20 kV	20 kV
Beam current	120 mA	125 mA	125 mA
Beam hole diam	190 μm	205 μm	225 μm
Small Sig. Gain	14 dB*	31 dB	37 dB
Bandwidth	15.5 GHz*	7 GHz	6 GHz
Max Power Out	63 W*	140 W	240 W
No. of gaps	64	93	29+47 [†]

(*measured quantity; [†]two sections with sever)

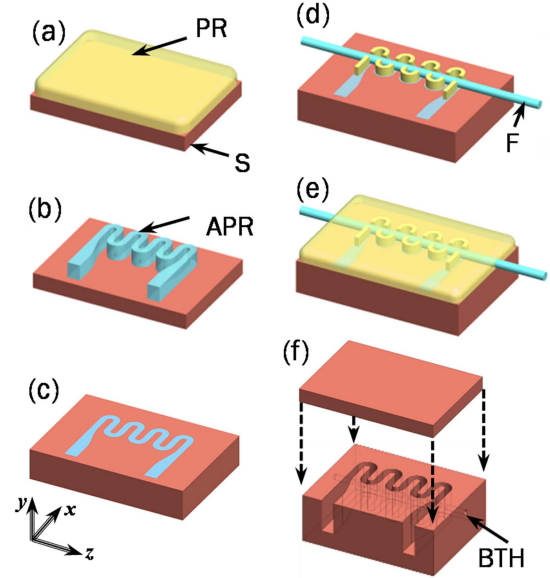


Figure 1. The two-layer UV-LIGA microfabrication process: (a) SU-8 photoresist (PR) is applied to a copper substrate. (b) SU-8 mold after UV patterning. (c) After electroforming first layer of copper. (d) SU-8 filament alignment posts patterned to guide polymer monofilament F to hold the size, shape and location of the electron beam tunnel. (e) Embed filament and posts in SU-8 and repeat steps (b)-(c). (f) Remove SU-8 and filament, braze flat lid on. APR: activated photoresist, BTH: beam tunnel hole.

Circuit Microfabrication

The microfabrication method involves patterning SU-8 photoresist on a copper substrate to create a high-precision, quasi-3D mold around which copper is electroformed. A precision extruded, UV-transparent monofilament embedded in the SU-8 creates the final shape of the beam tunnel, mitigating the need for sinker EDM, drilling, or other limited methods to create that very high aspect ratio hole (~100:1). The microfabrication process is shown in Fig. 1, utilizing two layers with a UV-transparent polymer monofilament embedded into the SU-8 in the second layer to create a 3D mold [2]. Due to the polymer's ability to be drawn down, the filament can simply be pulled out of the circuit after electroforming at ~100 °C. The SU-8 is removed by a Downstream Chemical Etching machine by Muegge, GmbH. The circuit is completed by brazing on a simple flat lid.

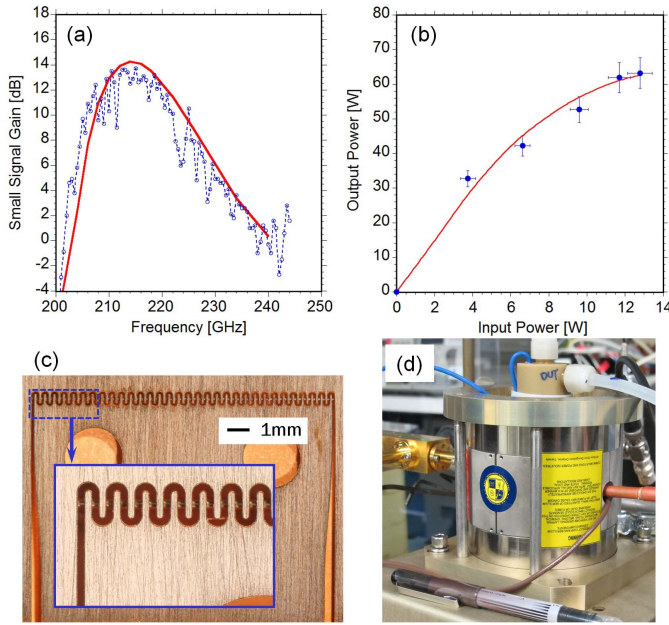


Figure 2. Results from the 220 GHz TWT. (a) Small signal circuit gain (dotted blue, circles) and simulation in the NRL 3D GPU PIC code Neptune [3] (solid red). (b) Power drive curve results at 214.5 GHz achieving 63W output power (blue dots) and Neptune simulation (solid red). (c) The microfabricated circuit prior to brazing on a flat lid. (d) Completed tube under hot test.

220 GHz TWT Demonstration

The 220 GHz TWT device was based on spare parts from a commercially available CPI VKY2444T G-band Extended Interaction Klystron (EIK) amplifier capable of 5W CW operation and 300 MHz bandwidth. Even considering the constraints imposed by the existing parts, our TWT bested this COTS EIK performance by a factor of 12x in power and 50x in bandwidth for the same size, weight and prime power by using a serpentine waveguide (SWG) interaction circuit. It was the first ever demonstration of a UV-LIGA fabricated circuit for a vacuum electron device.

Figure 2 summarizes the hot test results from the 220 GHz SWG TWT, the first vacuum electronic amplifier to use a circuit microfabricated by UV-LIGA [4]. The small-signal circuit gain peaked at 14 dB (excluding the input and output waveguide losses totaling 2.9 dB) at 11.7 kV and 104 mA. Approximately 15 GHz (7%) of small signal bandwidth was achieved. The maximum output power measured at the output flange was 63 W at 12.1 kV and 118 mA. Due to output waveguide losses of 1.0 dB, the power generated by the circuit is estimated to be 79 W. At the maximum output power level, 86% beam transmission was obtained through the 183 μ m diameter round beam tunnel hole. Because of the limited magnetic field length, the saturated gain was limited, requiring 13 W of input power from a G-band oscillator tube to reach full power. A photo of the completed compact tube under test is also shown.

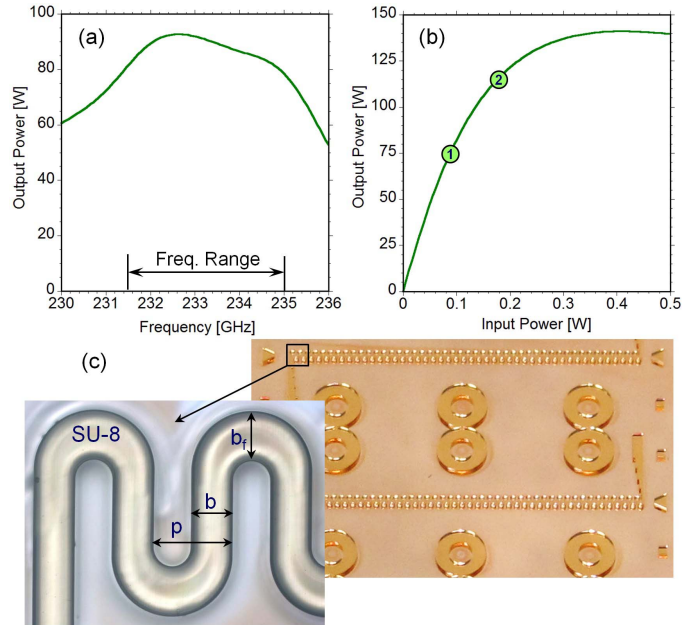


Figure 3. (a) Predicted circuit output power versus frequency assuming 113 mW input power showing 90 W output power expected. (b) Power drive curve at 232 GHz with markers representing (1) Expected operating point with a 100 mW solid state source driver, and (2) a 200 mW source, after accounting for waveguide losses. (c) Initial SU-8 structure of hybrid SWG circuit at 233 GHz, showing $b \neq b_f$.

233 GHz TWT Development

One shortcoming of the 220GHz TWT was that the gain of the TWT was under 10 dB when achieving >50 W output power, so a second vacuum tube was required as a driver. In order to operate from a solid state source directly supplying only 100 mW, closer to 30 dB of gain is needed. At high gain, however, oscillations are likely unless the circuit is “severed” into two sections. The sever causes the whole device to need a longer flat magnetic field length L for the electron beam transport, but the total weight of the magnet scales approximately as L^x , where x is between 2.5 and 3. Therefore, it is desirable to keep the circuit as short as possible. Figure 3 shows an innovative “hybrid” SWG concept wherein the waveguide gap size b is different from the gap size in the fold b_f [5]. This subtle change alters the dispersion relation and allows stable operation at over 30 dB of gain from a single, unsevered and uncoated section. This achievement is due in part to the relatively high mmW losses at these frequencies in the circuit, which act as a stabilizing mechanism. The circuit is being fabricated using the embedded polymer filament technique in three SU-8 layers with a laser pattern generator, which produces more reliable features than the previous flood source and photomask method used on the 220 GHz TWT.

Figure 4 illustrates the difference in techniques using the laser versus the flood source and photomask. Since the laser is a non-contact method it is capable of producing more accurate features repeatedly, and the spot size is very small

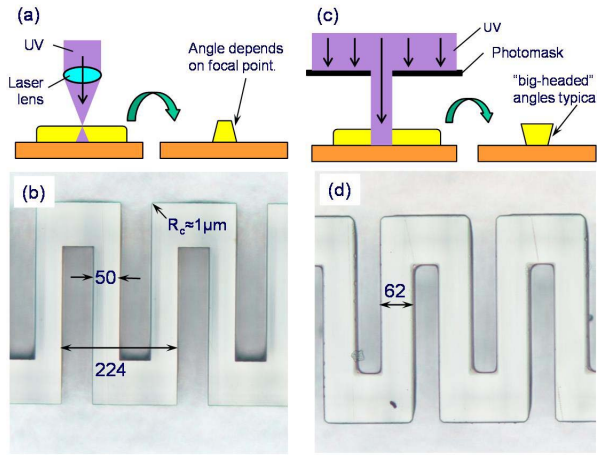


Figure 4. Comparison of laser to flood source with a 670GHz test circuit: (a) The laser method uses a focused beam with adjustable focus depth and (b) gives very sharp features on the top surface down to 1 μ m radius, but the resolution at the bottom depends on SU-8 thickness. (c) The flood source method gives lower resolution (d), but maintains the resolution through very thick SU-8 layers.

at only 3 μ m in diameter. However, because the laser is focused, it naturally spreads beyond the focal point, leading to lower resolution at the bottom of the SU-8 than the top. For a 300 μ m thick layer, the sharpest corner is about 8-10 μ m radius at the bottom and only \sim 2 μ m at the top. With adjustment of the focal depth, the optimal focal depth being about half way down into the SU-8, a good compromise in top/mid/bottom resolution can be reached. For the flood source method, there are inevitable gaps between the photomask and SU-8, leading to a loss of resolution. But the flood source beam is well collimated, so this resolution is the same throughout even very thick SU-8 layers.

Figure 5 shows a sweep of amplifier frequency response at various beam voltages showing that the TWT can potentially produce significant output power up to 245 GHz by reducing the beam voltage. These simulations were performed in the NRL fast design code TESLA-FW [6].

The electron gun generates an electron beam with nominal parameters of 20 kV at 124 mA. In addition to employing a mod-anode for varying the beam current, an additional focus electrode allows the current to vary from about 108 mA to 142 mA without defocusing (Figure 6). This variability is important because small errors in circuit fabrication tolerance could enhance the proclivity to oscillation, or if there is no oscillation, the output power and gain could be increased substantially beyond simulated values until an oscillation appears.

The vacuum window assembly uses a BeO ceramic disk and is predicted to achieve 35 GHz (15%) bandwidth at better than -20 dB reflection, easily meeting the requirements of the design (Figure 7). The predicted weight of the completed tube is approximately 20 lbs including the

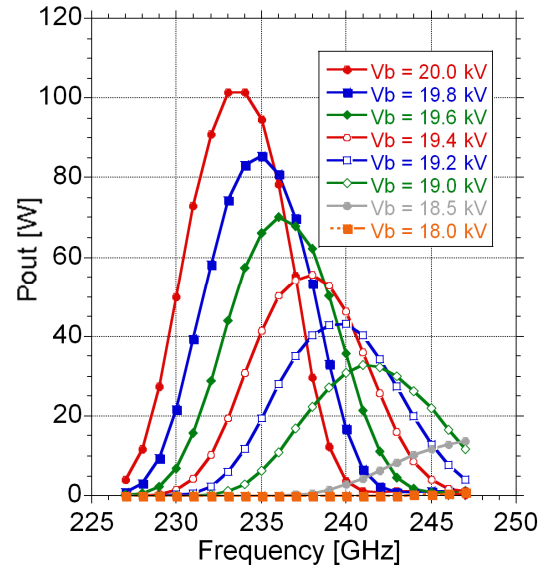


Figure 5. Simulations in the NRL code TESLA-FW [6] of the predicted TWT performance over a range of electron beam voltages. Broader bandwidth is obtainable at higher center frequencies with a sacrifice of output power. Input power is a constant 113 mW with 124 mA beam current for all cases.

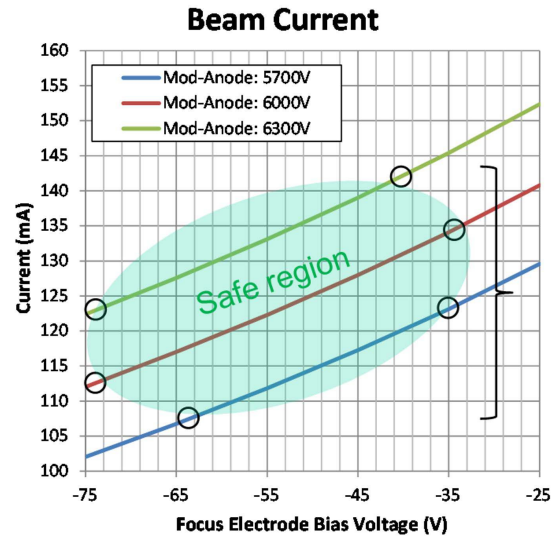
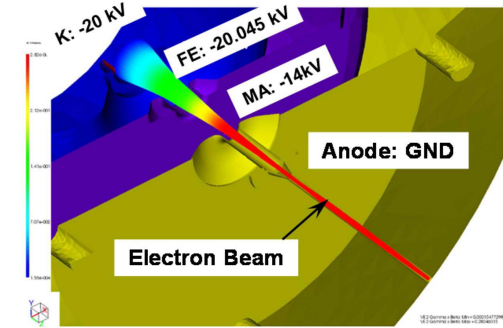


Figure 6. (Top) 3D model of the electron gun in the NRL code MICHELLE. K: Cathode, FE: Focus electrode, MA: Mod-anode. (Bottom) Predicted "safe" operating beam current of about 108-142 mA with <0.1mA intercepted electron current.

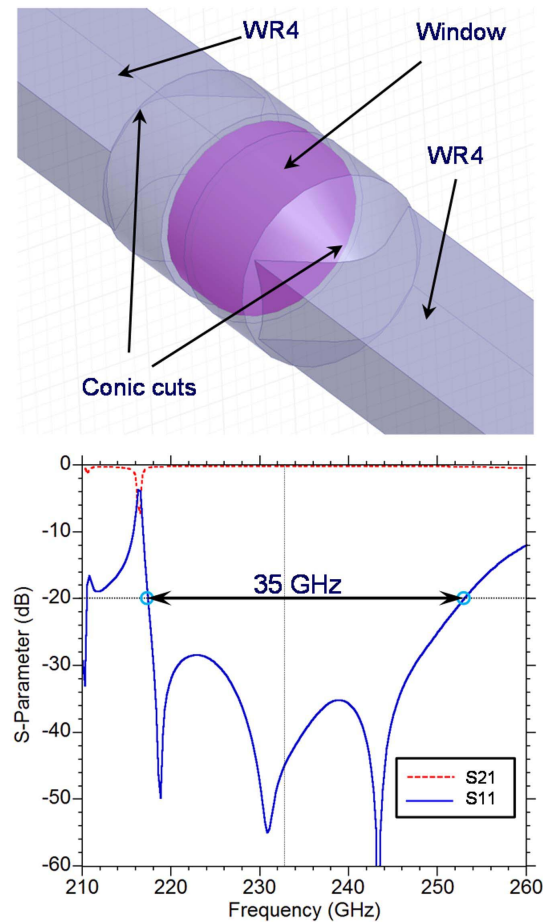


Figure 7: (Top) view of the vacuum window model in HFSS during simulation. The disc-shaped window resides between two conic sections cut into WR4 waveguides. (Bottom) Predicted optimal window performance showing over 35 GHz of bandwidth in simulation.

magnet focusing system, collector and water cooling jacket. Both this tube and the W-band tube use the same high-performance electron gun system design, reducing the engineering burden.

W-Band (94 GHz) TWT Development

Figure 8 shows predicted performance for a 2-stage W-band SWG TWT producing ~250 watts CW output power. By varying the input power over the frequency range, 6 GHz (6%) of 3 dB bandwidth is achievable using a ≤ 1 W solid state driver. The design features a sever between the two amplification stages to achieve high small-signal gain of 37 dB. The outputs from the sever waveguides feed into water-cooled matched loads that measured better than -25 dB reflection. The RF window design is predicted to have a bandwidth of 13 GHz (14%). The circuit is being fabricated using the laser and the embedded polymer UV-LIGA microfabrication technique with 4 layers to reach the final thickness of 1700 μm .

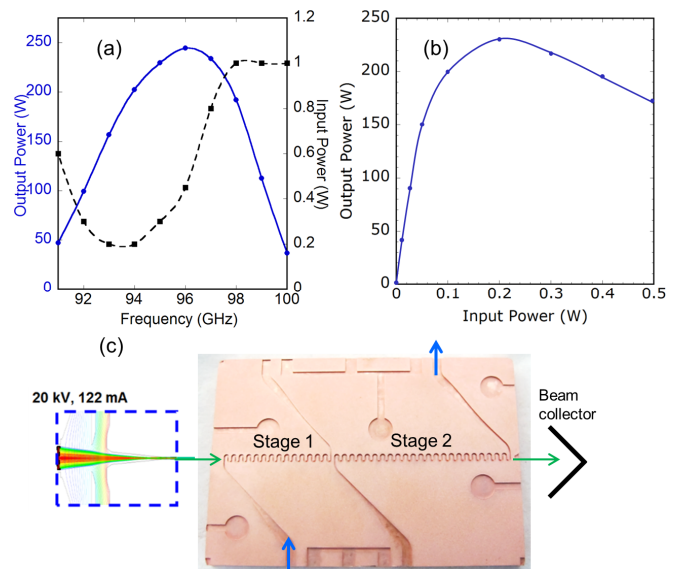


Figure 8. (a) W-band 2-stage TWT predicted performance versus frequency at the saturated regime (maximum input power, 1W) with ~6 GHz of 3dB bandwidth at 20 kV, 124 mA. (b) Simulated power drive curve at 94 GHz. (c) Initial circuit fabrication using UV-LIGA in copper with the embedded polymer monofilament technique.

Acknowledgement

This work is sponsored by the U.S. Office of Naval Research. The authors wish to thank R. E. Myers, B. S. Albright, F. N. Wood, and L. N. Blankenship for their assistance.

References

1. J. H. Booske, *et al.*, "Vacuum Electronic High Power Terahertz Sources," *IEEE Trans. on THz Sci./ Techn.*, Vol. 1, No. 1, pp. 54-75, Sept. 2011.
2. C. D. Joye, *et al.*, "Microfabrication of fine electron beam tunnels using UV-LIGA and embedded polymer monofilaments for vacuum electronics," *J. of Micromech./ Microeng.*, Vol. 22, p.015010, Jan. 2012.
3. S. J. Cooke, *et al.*, "GPU-accelerated 3D large-signal device simulation using the particle-in-cell code 'Neptune'," *IEEE 13th Int. Vac. Electron. Conf.*, pp. 21-22, April 2012.
4. C. D. Joye, *et al.*, "Demonstration of a High Power, Wideband 220 GHz Traveling Wave Amplifier Fabricated by UV-LIGA," *IEEE Trans. Electron Dev.*, Vol. 61, No. 6, pp. 1672-1678, June 2014.
5. K. T. Nguyen, *et al.*, "Design Methodology and Experimental Verification of Serpentine/Folded-Waveguide TWTs," *IEEE Trans. Electron Dev.*, Vol. 61, No. 6, pp. 1679-1686, June 2014.
6. I. A. Chernyavskiy, A. N. Vlasov, B. Levush and T. M. Antonsen, Jr., "2D Modeling of TWTs Based on Serpentine and Folded Waveguide Structures," *IEEE Conference on Plasma Science (ICOPS)*, 2012, Edinburgh, Scotland, UK, July 8-12, 2012.